Korringa and phonon nuclear-spin–lattice relaxation in metallic arsenic

J. M. Keartland, G. C. K. Fölscher,* and M. J. R. Hoch
Department of Physics, University of the Witwatersrand, Johannesburg, P.O. Wits 2050, South Africa
(Received 23 September 1991)

The spin-lattice relaxation time (T_1) in arsenic (^{75}As nucleus; $I=\frac{3}{2}$) has been measured, using pulsed nuclear-quadrupole-resonance methods, as a function of temperature from 4 to 596 K. The results show that T_1 follows the Korringa relation ($T_1T=$const) for temperatures below the Debye temperature ($\Theta_D=282$ K). Above Θ_D the data break away from this relation, and the measured T_1 is shorter than that predicted by a nucleus-carrier relaxation model. Previous calculations of nucleus-carrier spin-flip transition probabilities involving a spherical Fermi surface (FS) have been extended to the nonspherical FS of arsenic. Modified expressions have been derived using a spheroidal approximation to the FS pockets. The carrier wave functions are approximated by free-atom wave functions. These calculations can account for the magnitude of measured nucleus-carrier interactions at low temperatures, and predict the usual Korringa law for the temperature dependence. The experimental results above Θ_D can be accounted for using both nucleus-carrier processes ($\propto T$) and nucleus-phonon processes ($\propto T^2$).

I. INTRODUCTION

The electronic properties of the rhombohedral semimetals (arsenic, antimony, and bismuth) have attracted a great deal of interest over the years.[1] This interest centers on the intermediate position these materials occupy between good metals and insulators. The carrier concentration of the semimetals is typically a few orders of magnitude lower than that of good metals. In contrast to semiconductors, the conductivity increases as the temperature decreases. The semimetals are compensated metals; both electrons and holes are present as current carriers. The position of the semimetals in group V of the Periodic Table means that the carriers are likely to exhibit both *s*-wave and *p*-wave properties. The elastic properties of these materials have also attracted interest. The existence of optical modes in the vibration spectra is a common feature to all three semimetals.[2]

Previous measurements[3–5] of nuclear-spin–lattice relaxation effects in arsenic and antimony have suggested that nucleus-carrier interactions play an important role. This is particularly true for temperatures lower than ambient. At higher temperatures the data for antimony indicate that another relaxation mechanism becomes important, and it has been suggested that this is a nucleus-phonon process.

This paper reports on experimental data for the spin-lattice relaxation time (T_1) in metallic arsenic for the temperature range 4–596 K. We present calculations of the nucleus-carrier transition rates, allowing for the nonspherical Fermi surface of arsenic, which account for the observed T_1 at temperatures below the Debye temperature, Θ_D. The data above Θ_D are explained by including a contribution that takes into account the acoustic phonons. The combined model shows excellent agreement with the experimental data.

II. THEORETICAL CONSIDERATIONS

A. Quadrupolar Hamiltonian and the rate equation

Rhombohedral arsenic crystallizes in the A_7 structure.[6] This gives rise to an axially symmetric electric-field gradient (efg) at each nuclear site. The carriers at the Brillouin-zone boundary and the ionic cores contribute to the efg.[7] The interaction of the efg with the electric quadrupole moment of the nucleus may be described by the axially symmetric quadrupolar Hamiltonian[8]

$$\mathcal{H}_Q=\frac{1}{4\pi\epsilon_0}\frac{e^2qQ}{4I(2I-1)}(3I_z^2-I^2)\ , \tag{1}$$

where $eq/4\pi\epsilon_0$ is the efg, Q is the nuclear-quadrupole moment, I_z and I^2 are nuclear-spin angular momentum operators, I is the nuclear-spin quantum number, and ϵ_0 is the permittivity of the vacuum.

The rate equations describing spin-lattice relaxation may be derived using the procedure developed by MacLaughlin, Williamson, and Butterworth.[9] Suppose that p_m is the deviation of the mth nuclear-spin level population from equilibrium, and that $P_m=p_m+p_{-m}$. If u_m is defined as

$$u_m=P_m-P_{m-1}\ , \tag{2}$$

then the rate equations for the quadrupolar system may be found. The probabilities of the possible transitions contributing to relaxation are

$$W^M_{m,m'}=W_m|\langle m'|I_\pm|m\rangle|^2\ , \tag{3a}$$

$$W^{Q1}_{m,m'}=W_{Q1}|\langle m'|I_\pm I_z+I_zI_\pm|m\rangle|^2\ , \tag{3b}$$

$$W^{Q2}_{m,m'}=W_{Q2}|\langle m'|I^2_\pm|m\rangle|^2\ , \tag{3c}$$

where the quantity W_m is a magnetic ($\Delta m = \pm 1$) coupling and W_{Q1}, W_{Q2} are quadrupolar ($\Delta m = \pm 1, \pm 2$) couplings. These quantities contain information on the spin-lattice interactions. The nuclear quadrupolar spin system evolves with time according to the matrix differential equation

$$\frac{d\mathbf{u}}{dt} = A\mathbf{u} , \tag{4}$$

subject to the appropriate initial conditions. A is known as the relaxation matrix, and for an $I = \frac{3}{2}$ system is given by

$$A = -(6W_m + 24W_{Q1} + 12W_{Q2}) .$$

The spin-lattice relaxation time may then be defined as

$$\frac{1}{T_1} = 6W_m + 24W_{Q1} + 12W_{Q2} . \tag{5}$$

B. Nucleus-carrier interactions

The interaction of the nucleus and the carriers may be described by the Hamiltonian[10]

$$\mathcal{H}_s = \mathcal{H}_m + \mathcal{H}_q , \tag{6}$$

where $\mathcal{H}_m$ and $\mathcal{H}_q$ refer, respectively, to magnetic and quadrupolar interactions, which give rise to spin-lattice relaxation. The Fermi-surface parameters and carrier wave functions are important factors in the description of these effects in the semimetals, and are discussed below. Nucleus-carrier transition rates are calculated at 77 K for each of the nucleus-carrier interactions.

1. Magnetic interactions

The Hamiltonian $\mathcal{H}_m$ may be written in terms of the spherical polar coordinates of the carrier displacement with respect to the nucleus (r, Θ, ϕ)

$$\mathcal{H}_m = \frac{\mu_0}{4\pi} \sum_{i=-1}^{1} \gamma_i B_i , \tag{7}$$

where

$$\gamma_0 = g\mu_N I_z , \quad \gamma_{\pm 1} = g\mu_N I_{\pm} ,$$

$$B_0 = 2\mu_B \left[\frac{L_z}{r^3} + \frac{s_z(3\cos^2\Theta - 1)}{r^3} + \frac{3\sin\Theta\cos\Theta(s_+ e^{-i\phi} + s_- e^{+i\phi})}{2r^3} + \frac{8\pi}{3} s_z \delta(\mathbf{r}) \right] ,$$

$$B_{\pm 1} = \mu_B \left[\frac{L_{\mp}}{r^3} - \frac{s_{\mp}(3\cos^2\Theta - 1)}{2r^3} + \frac{3s_z \sin\Theta\cos\Theta e^{\mp i\phi}}{r^3} + \frac{3s_{\pm}\sin^2\theta e^{\mp 2i\phi}}{2r^3} + \frac{8\pi}{3} s_{\mp}\delta(\mathbf{r}) \right] ,$$

and

$$L_z = -i\frac{\partial}{\partial\phi} , \quad L_{\pm} = e^{\mp i\phi}\left[\frac{\partial}{\partial\Theta} + i\cot\Theta\frac{\partial}{\partial\phi} \right] .$$

All of the symbols above have their usual meaning. The terms involving $I_{\pm}$ give rise to spin-lattice interactions of the form

$$\langle s_z \mp 1, m \pm 1 | \mathcal{H}_m | s_z, m \rangle = \frac{\mu_0}{4\pi}\mu_B g\mu_N \left[\frac{8\pi}{3}\delta(\mathbf{r}) - \frac{3\cos^2\Theta - 1}{2r^3} \right] \sqrt{w_m} , \tag{8a}$$

$$\langle s_z \pm 1, m \pm 1 | \mathcal{H}_m | s_z, m \rangle = \frac{\mu_0}{4\pi}\mu_B g\mu_N \left[\frac{3\sin^2\Theta e^{\mp 2i\phi}}{2r^3} \right] \sqrt{w_m} , \tag{8b}$$

$$\langle s_z, m \pm 1 | \mathcal{H}_m | s_z, m \rangle = \frac{\mu_0}{4\pi}\mu_B g\mu_N \left[\frac{L_{\mp}}{r^3} + \frac{3s_z\sin\Theta\cos\Theta e^{\mp i\phi}}{2r^3} \right] \sqrt{w_m} , \tag{8c}$$

where $w_m = |\langle m \pm 1 | I_{\pm} | m \rangle|^2 = (I \pm m)(I \mp m + 1)$.

2. Quadrupolar interactions

The Hamiltonian $\mathcal{H}_q$ may also be written in terms of the displacement of the carrier with respect to the nucleus

$$\mathcal{H}_q = \frac{e}{4\pi\epsilon_0} \sum_{i=-2}^{2} Q_i V_i , \tag{9}$$

where

$$V_0=\frac{3\cos^2\Theta-1}{2r^3}\ ,\quad Q_0=\frac{eQ}{2I(2I-1)}(3I_z^2-I^2)\ ,$$

$$V_{\pm1}=\pm\left[\frac{3}{2}\right]^{1/2}\frac{\sin\Theta\cos\Theta e^{\pm i\phi}}{r^3}\ ,\quad Q_{\pm1}=\pm\left[\frac{3}{2}\right]^{1/2}\frac{eQ}{2I(2I-1)}(I_zI_\pm+I_\pm I_z)\ ,$$

$$V_{\pm2}=\left[\frac{3}{8}\right]^{1/2}\frac{\sin^2\Theta e^{\pm2i\phi}}{r^3}\ ,\quad Q_{\pm2}=\left[\frac{3}{2}\right]^{1/2}\frac{eQ}{2I(2I-1)}I_\pm^2\ .$$

The above symbols again have their usual meaning. The interaction gives rise to $\Delta m=\pm1$ and $\Delta m=\pm2$ transitions, and leaves the carrier spin unchanged. The two transitions are

$$\langle s_z,m\pm1|\mathcal{H}_q|s_z,m\rangle=\frac{3e^2Q}{4I(2I-1)}\frac{\sin\Theta\cos\Theta e^{\pm i\phi}}{r^3}(w_q^{\pm1})^{1/2}\ , \tag{10a}$$

$$\langle s_z,m\pm2|\mathcal{H}_q|s_z,m\rangle=\frac{3e^2Q}{8I(2I-1)}\frac{\sin^2\Theta e^{\pm2i\phi}}{r^3}(w_q^{\pm2})^{1/2}\ , \tag{10b}$$

where

$$w_q^{\pm1}=|\langle m\pm1|I_\pm I_z+I_zI_\pm|m\rangle|^2=(2m\pm1)^2[I(I+1)-m(m\pm1)]\ ,$$

$$w_q^{\pm2}=|\langle m\pm2|I_\pm^2|m\rangle|^2=(I\pm m)(I\mp m+1)(I\pm m+1)(I\mp m+2)\ .$$

In the next section the effect of Fermi-surface characteristics and choice of carrier wave function on the nucleus-carrier transition probabilities will be examined.

3. *Fermi-surface characteristics and the carrier wave function*

The Fermi surface (FS) of arsenic has been studied using theoretical[11] and experimental[12–14] approaches. The electrons and holes are found around the L and T points of crystal symmetry, respectively, in well-defined pockets, which may be approximated by ellipsoids.[14] The FS parameters determined by Ih and Langenberg[14] are displayed in Table I. The effective-mass data show that $m_x\simeq m_z\ll m_y$, so that the ellipsoids may be approximated as spheroids. This approximation simplifies the analysis greatly, and is not expected to have a significant effect on the results. It employs the relation

$$\bar{m}_x=\bar{m}_z=\frac{m_x+m_z}{2}\ . \tag{11}$$

The carrier wave function must reflect the s- and p-wave nature of the carriers in the semimetals. The chosen wave function is based on expressions used by Bardeen,[15] Korringa,[16] and Mitchell,[17] and is written as

$$\psi_{\mathbf{k}}(\mathbf{r})=u_{\mathbf{k}}(r)+i\mathbf{k}\cdot\mathbf{r}v(r)\ , \tag{12}$$

where $u_{\mathbf{k}}(r)$ and $v(r)$ are s- and p-wave radial wave functions. Using this wave function, it is possible to determine the matrix elements for transitions from a carrier state $\mathbf{k}$ to a carrier state $\mathbf{k}'$

$$\langle\mathbf{k}'|\mathcal{H}_s|\mathbf{k}\rangle=\int\psi_{\mathbf{k}'}^*(\mathbf{r})\mathcal{H}_s\psi_{\mathbf{k}}(\mathbf{r})d^3r\ . \tag{13}$$

In order to determine these matrix elements the angular coordinates are removed by integrating over a sphere. The following matrix elements are found:

$$\langle\mathbf{k}',s_z\mp1,m\pm1|\mathcal{H}_m|\mathbf{k},s_z,m\rangle=\left[\frac{F}{2}(\mathbf{k}'\cdot\mathbf{k}-3k_z'k_z)+G\right]\sqrt{w_m}\ , \tag{14a}$$

$$\langle\mathbf{k}',s_z\pm1,m\pm1|\mathcal{H}_m|\mathbf{k},s_z,m\rangle=\frac{3F}{2}[(k_x'k_x-k_y'k_y)\mp i(k_x'k_y+k_y'k_x)]\sqrt{w_m}\ , \tag{14b}$$

$$\langle\mathbf{k}',s_z,m\pm1|\mathcal{H}_m|\mathbf{k},s_z,m\rangle=\frac{F}{3}[(k_y'k_z+k_z'k_y)\pm i(k_z'k_x-k_x'k_z)]\sqrt{w_m}+3Fs_z[(k_x'k_z+k_z'k_x)\mp i(k_y'k_z+k_z'k_y)]\sqrt{w_m}\ , \tag{14c}$$

$$\langle\mathbf{k}',s_z,m\pm1|\mathcal{H}_q|\mathbf{k},s_z,m\rangle=H[(k_x'k_z+k_z'k_x)\pm i(k_y'k_z+k_z'k_y)]\sqrt{w_q^{\pm1}}\ , \tag{14d}$$

$$\langle\mathbf{k}',s_z,m\pm2|\mathcal{H}_q|\mathbf{k},s_z,m\rangle=H[(k_x'k_x-k_y'k_y)\pm i(k_x'k_y+k_y'k_x)]\sqrt{w_q^{\pm2}}\ , \tag{14e}$$

where

$$F=\frac{\mu_0}{4\pi}\frac{\mu_B g\mu_N}{5}\int\frac{|v(r)|^2}{r}d^3r\ ,$$

$$G=\frac{\mu_0}{4\pi}\mu_B g\mu_N\frac{8\pi}{3}u_k(0)u_{k'}(0)\ ,$$

$$H=\frac{1}{4\pi\epsilon_0}\frac{e^2qQ}{10I(2I-1)}\int\frac{|v(r)|^2}{r}d^3r\ .$$

The probability of a transition from a nuclear spin state m to a nuclear spin state m', with a simultaneous transition from a lattice state $\mathbf{k},\mathbf{s}$ to a lattice state $\mathbf{k}',\mathbf{s}'$, may be determined as follows:

$$W_{m',\mathbf{k}',\mathbf{s}';m,\mathbf{k},\mathbf{s}}=\frac{2\pi}{\hbar}\sum_{\mathbf{k},\mathbf{k}'}|\langle m,\mathbf{k},\mathbf{s}|\mathcal{H}_s|m',\mathbf{k}',\mathbf{s}'\rangle|^2\delta(E^{\mathbf{s}'}_{\mathbf{k}'}-E^{\mathbf{s}}_{\mathbf{k}}+E_{m'}-E_m)\ , \tag{15}$$

where the sum is over occupied ($\mathbf{k}$) and unoccupied ($\mathbf{k}'$) carrier momentum states. For a metal this means that only momentum states within an energy kT of the Fermi energy are involved. The sums are converted to integrals in k-space in the usual way.[16,17] The integrals depend on the shape of the FS pockets, and the details of determining them for the spheroidal FS approximation are given elsewhere.[18] Carrier-carrier interactions were ignored.

4. *Calculation of the transition probabilities*

The expressions developed in Sec. IIB 3 to describe the various possible nucleus-carrier interactions may be divided into contact and noncontact interactions. Contact interactions arise from interactions with s-wave carriers, while noncontact interactions are due to the p-wave carriers. The contact terms involve the probability of finding an s-wave carrier at the nucleus, $|u_k(0)|^2$, while the noncontact terms depend on the quantity $\int[|v(r)|^2/r]d^3r$. These quantities were calculated using the free-atom wave functions of Herman and Skillman.[19] The contact interactions are magnetic in origin, but the noncontact terms may arise from both magnetic and quadrupolar interactions.

The quantities W_m, W_{Q1}, and W_{Q2} may be identified with the coefficients of w_m, $w_q^{\pm1}$, and $w_q^{\pm2}$ in the full expressions for the nucleus-carrier transition probabilities. For instance, the expression for W_{Q1} is

$$W_{Q1}=\frac{2\pi}{\hbar}H^2\sum_{\mathbf{k},\mathbf{k}'}[(k_x'k_z+k_z'k_x)^2+(k_y'k_z+k_z'k_y)^2]\delta(E_{k'}+E_{m'}-E_k-E_m)\ , \tag{16}$$

where H is defined in Eq. (14). The sum is to be converted to an integral as indicated above.

The magnetic interaction is made up of contact (c) and noncontact (nc) terms

$$W_m=W_m^{\mathrm{c}}+W_m^{\mathrm{nc}}\ . \tag{17}$$

The contact term for each carrier (electrons or holes) may be found explicitly by considering interpocket scattering. The expression for each type of carrier is given by

$$W_m^{\mathrm{c}}=\frac{2\pi}{\hbar}\left[\frac{\mu_0}{6}\mu_B g\mu_N\right]^2\left[\frac{Nv_0}{\sqrt{2}\pi^2\hbar^3}\right]^2E_F m_x m_y m_z|u_k(0)|^4kT\ , \tag{18}$$

where N is the number of pockets,and m_x,m_y,m_z are the carrier effective masses.

The various transition rates have been calculated at 77 K and are tabulated in Table II. The antishielding factor of Feiock and Johnston[20] was included in the quadrupolar terms. It should be noted that all of the above transition rates are directly proportional to the absolute temperature.

TABLE I. Fermi surface parameters for arsenic determined using cyclotron resonance techniques and an ellipsoidal approximation (Ref. 14). The effective masses displayed here are in units of the rest mass of the electron.

	Electrons	Holes
m_x	0.121	0.122
m_y	1.180	1.040
m_z	0.138	0.081
Θ_T	83.6°	38°
E_F (eV)	0.210	0.178

C. Nucleus-phonon interactions

The theory outlined in this section is similar to that given by Abragam,[10] which does not take into account the symmetry of the lattice, and involves only acoustic

TABLE II. Nucleus-carrier transition rates at 77 K. The results for the quadrupolar contributions include Sternheimer antishielding effects.

	W_m^{c} (s^{-1})	W_m^{nc} ($10^{-7}\,\mathrm{s}^{-1}$)	W_{Q1} ($10^{-8}\,\mathrm{s}^{-1}$)	W_{Q2} ($10^{-8}\,\mathrm{s}^{-1}$)
electrons	0.56	3.20	1.35	7.95
holes	0.98	2.96	10.4	3.69

phonons. Calculations of nucleus-phonon interactions have been undertaken for the NaCl lattice[21] and the ZnS lattice.[22] No calculations for the A_7 structure have been reported.

The dominant term for nucleus-phonon relaxation processes is due to the Raman interaction, whereby a phonon of frequency ω is emitted and a phonon of frequency ω' is absorbed. The probability of a transition of a nucleus from a state m to a state m' in the Raman process is calculated using the Debye approximation to the phonon density of states. In order to obtain the total transition probability, the expression for the probability of the simultaneous transition must be summed over all possible frequencies of the absorbed phonon. This sum may be converted to an integral over all phonon frequencies up to the Debye frequency, ω_D. Using Planck's Law for the phonon occupation number, and inserting a quantity appropriate to the symmetry of the lattice, the final expressions for the nucleus-phonon transition rates W_{Q1} and W_{Q2} are given by

$$W_{Q\mu}=\frac{243\pi}{16}\left[\frac{eQF_\mu\hbar}{I(2I-1)mv^2}\right]^2 \times\int_0^{\omega_D}\frac{\exp(\beta\hbar\omega)}{[\exp(\beta\hbar\omega)-1]^2}\frac{\omega^6}{\omega_D^6}d\omega\ , \tag{19}$$

where $\beta=1/kT$, μ takes on the values 1 and 2, the quantities F_μ depend on the lattice symmetry, v is the velocity of sound in the crystal, and m is the atomic mass of the sample. The integral may be rewritten in terms of Θ_D and the temperature T in order to determine the temperature dependence of the quantities W_{Q1} and W_{Q2} as follows:

$$W_{Q1,Q2}(T)\propto T^7\int_0^{\Theta_D/T}\frac{x^6e^x}{(e^x-1)^2}dx\ . \tag{20}$$

An order-of-magnitude estimate of the nucleus-phonon transition probabilities is not possible, because the quantities F_μ are not available for the A_7 structure.

III. EXPERIMENTAL DETAILS

High-purity (99.9999%) arsenic shot was obtained from Koch-Light, UK. The samples were crushed to 25 μm, and annealed for 48 h at a temperature of 400 °C. Following annealing, the material was sieved gently to remove sintered aggregates. The sample was then sealed in a Pyrex ampoule under vacuum. This prevented oxidation through contact with the atmosphere, since crushed arsenic oxidizes readily.

A standard variable-frequency, coherent, pulsed nuclear-quadrupole-resonance (NQR) spectrometer operating at a frequency ν_0 in the range 21–24 MHz was used to make quadrupolar spin-echo measurements. The frequency source used was a crystal-locked Hewlett Packard HP3335A synthesizer operating at frequency $\frac{1}{2}\nu_0$. A Tektronix 468 digital storage oscilloscope with signal averaging capability was used for data capture. Baseline corrections and a nine-point smoothing routine were applied to the data, using a Hewlett Packard microcomputer, before the amplitude of the spin echo was measured.

Measurements of spin-lattice relaxation were made over a wide temperature range (4–596 K). Temperature control was achieved using a helium cryostat over the range 4–60 K. A germanium thermometer was used at the lower temperatures in the helium range, while an Oxford Instruments linear temperature sensor was used for control and measurement at the higher temperatures. Temperatures were controlled and measured to within ±1 K. Above 60 K various fixed-temperature baths were used. Temperatures up to 600 K were achieved using a furnace probe, with a copper-constantan thermocouple for control and measurement.

IV. EXPERIMENTAL RESULTS AND DISCUSSION

The relaxation data are expected to follow a relation of the form

$$1-\frac{M(t)}{M_0}=A\exp\left[-\frac{t}{T_1}\right] \tag{21}$$

where T_1 has been defined in Sec. II, $M(t)$ is the spin echo amplitude a time t after a saturating pulse, M_0 is the equilibrium amplitude of the spin echo, and A is a constant determined by the effect of the saturating pulse ($A\simeq1$). T_1 is extracted from a linear regression analysis of the relaxation data at each temperature. The results for T_1 as a function of temperature are displayed in Fig. 1. The straight line through the data is the result of fitting the Korringa relation to the low-temperature data ($T\leq88$ K), as indicated below. At higher temperatures the data show a departure from Korringa behavior, which suggests that another spin-lattice relaxation mechanism becomes important. It is proposed that this mechanism is a two-phonon (Raman) process of the type discussed in Sec. II C. The defining expression for T_1 in arsenic given in Sec. II A may be rewritten as

$$\frac{1}{T_1}=AT+BT^7\int_0^{\Theta_D/T}\frac{x^6e^x}{(e^x-1)^2}dx\ , \tag{22}$$

where the temperature dependence of the nucleus-carrier and nucleus-phonon interactions are derived in Sec. II. It

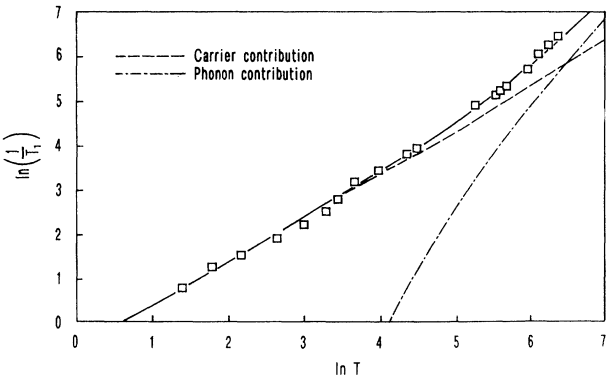

FIG. 1. Spin-lattice relaxation rate $1/T_1$ (T_1 in s) as a function of temperature $T(k)$ for arsenic. The curves shown are the result of fitting procedures described in the text.

is important to recall that the second term in Eq. (22) takes into account contributions from the acoustic phonons. No attempt to include the optical phonons is made here. The constants A and B are determined by fitting the relation (22) to the $T_1 - T$ data using the following procedure:

A is determined by fitting a straight line to the low-temperature ($T \leq 88$ K) data. This value for A is substituted into Eq. (22) and the value for B determined using a least-squares fitting procedure to all the data points shown in Fig. 1. The integral in Eq. (22) is determined numerically for each temperature using Simpson's rule.

The calculated T_1 values obtained using the above procedure are plotted together with the experimental data in Fig. 1. It can be seen that the model provides a plausible fit to the data.

Jellison and Taylor[3] have measured T_1 in rhombohedral arsenic in the temperature range 77–300 K. Our results are in good agreement with their results in this temperature range, and their measurement at 300 K shows evidence of deviation from the Korringa relation. In their data analysis they assumed that all relaxation was due to the contact magnetic interaction, and did not consider noncontact carrier processes, or phonon processes. We have presented a more detailed analysis of the experimental results, and have used details of the Fermi surface obtained by other workers. They also found evidence of impurity-dominated relaxation at 4.2 K in their high-purity sample, but we have not observed a similar effect. Measurements in high-purity arsenic[23] below 1 K indicate that the Korringa relation is obeyed down to a temperature of 150 mK.

Measurements of spin-lattice relaxation effects at low temperatures in antimony[4,5] indicate that noncontact carrier processes may make detectable contributions to relaxation in this temperature regime. The band structures and Fermi surfaces of arsenic and antimony show many common features, and it is likely that noncontact terms make important contributions in arsenic. The results of the calculations described in Sec. II and tabulated in Table II indicate that these contributions are several orders of magnitude smaller than the contact contribution. It is possible that the approximate wave function Eq. (12) may deviate markedly from the crystal wave function, particularly far away from the nucleus. In order to obtain a quantitative estimate of the effect of using crystal wave functions on the nucleus-carrier transition rates, the Knight shift has been calculated for antimony using Eq. (12). The details of this calculation are presented elsewhere.[18] A comparison of these results with the results of Hygh and Das[24] for antimony shows that the Knight shift due to the p-wave carriers is underestimated by approximately 10^3 if the free-atom wave functions are used. This implies that the noncontact nucleus-carrier interactions may be underestimated by approximately 10^6, and brings the calculated values to the same order of magnitude as the experimental results for antimony. The same arguments may apply to arsenic, but we are not aware of any calculation of the Knight shift for arsenic using good approximations to the crystal wave functions. Further work on the noncontact carrier effects should include approximate crystal wave functions. It is clear that the contact term plays the dominant role in spin-lattice relaxation at low temperatures.

Measurements of spin-lattice relaxation effects at temperatures above Θ_D in antimony[5] have indicated that Raman nucleus-phonon processes may make significant contributions. The present results indicate that this occurs in arsenic as well. The measured phonon densities of states[2] for arsenic and antimony have many common features. Two peaks are observed, corresponding to acoustic and optical modes. The Debye frequency ν_D of each of these materials lies close to the peak in the optical branch ($\nu_D = 5.9$ THz for arsenic and $\nu_D = 4.4$ THz for antimony). A more precise calculation of the Raman transition rates would involve using the measured phonon density of states and considerations of the lattice symmetry for the A_7 structure. Using a point charge approach, calculations of this type typically predict relaxation rates that are within one or two orders of magnitude of the measured rates. Such a calculation would therefore prove a useful comparison for the results of the fitting procedure described above. The predicted temperature dependence for temperatures above Θ_D would not, however, deviate markedly from the results of the simple model described in Sec. II C.

V. CONCLUSION

The nuclear spin-lattice relaxation time (T_1) in metallic arsenic has been measured over a wide temperature range. The data obtained using pulsed NQR techniques have been analyzed in terms of nucleus-carrier and nucleus-phonon processes, and have been fitted to theoretical expressions for the temperature dependence of these processes over the entire measured range.

In addition, we have presented calculations of the nucleus-carrier transition rates that take into account the nonspherical Fermi surface. A comparison of the experimental results with the calculated contact and noncontact terms shows that the contact term plays the dominant role in the low-temperature region. The results are also compared to experimental and theoretical results for the same processes in antimony. It is suggested that improved estimates of the crystal wave function will reveal that the noncontact terms may make important contributions to the measured relaxation rate at low temperatures.

For temperatures above Θ_D we suggest that nucleus-phonon Raman processes make significant contributions to the relaxation rate. Comparison of our results with previous results for antimony suggests that this behavior is characteristic of the Group V semimetals. Further investigations of this effect might focus on calculations of Raman transition rates for the A_7 structure.

ACKNOWLEDGMENTS

The authors gratefully acknowledge the technical assistance of Mr. P. van der Schyff. Financial assistance from the Foundation for Research Development is also acknowledged.

*Deceased.

[1]M. S. Dresselhaus, in *The Physics of Semimetals and Narrow Gap Semiconductors,* edited by D. E. Carter and R. T. Bate (Pergamon, London, 1971).

[2]H. R. Schöber and P. H. Dederichs, in *Numerical Data and Functional Relationships,* edited by K. -H. Hellewege and J. L. Olsen (Springer-Verlag, Berlin, 1981), Vol. 13.

[3]G. E. Jellison, Jr. and P. C. Taylor, Solid State Commun. **27**, 1025 (1978).

[4]R. R. Hewitt and D. E. MacLaughlin, J. Magn. Reson. **30**, 483 (1978).

[5]J. M. Keartland, G. C. K. Fölscher, and M. J. R. Hoch, Phys. Rev. B **43**, 8362 (1991).

[6]R. W. G. Wyckoff, *Crystal Structures* (Wiley, New York, 1963).

[7]S. N. Sharma, Phys. Lett. **57A**, 379 (1976).

[8]C. P. Slichter, *Principles of Magnetic Resonance* (Springer-Verlag, Berlin, 1980).

[9]D. E. MacLaughlin, J. D. Williamson, and J. Butterworth, Phys. Rev. B **4**, 60 (1971).

[10]A. Abragam, *The Principles of Nuclear Magnetism* (Oxford University Press, New York, 1968).

[11]P. J. Lin and L. M. Falicov, Phys. Rev. **142**, 441 (1966).

[12]M. G. Priestley, L. R. Windmiller, J. B. Ketterson, and Y. Eckstein, Phys. Rev. **149**, 472 (1966).

[13]A. P. Jeavons and G. A. Saunders, Proc. R. Soc. London, Ser. A **310**, 415 (1969).

[14]C. S. Ih and D. N. Langenberg, in *The Physics of Semimetals and Narrow Gap Semiconductors,* edited by D. E. Carter and R. T. Bate (Pergamon, London, 1971).

[15]J. Bardeen, J. Chem. Phys. **6**, 367 (1938).

[16]J. Korringa, Physica **16**, 601 (1950).

[17]A. H. Mitchell, J. Chem. Phys. **26**, 1714 (1957).

[18]J. M. Keartland, Ph.D. thesis, University of the Witwatersrand, Johannesburg, 1991.

[19]F. Herman and S. Skillman, *Atomic Structure Calculations* (Prentice-Hall, Englewood Cliffs, NJ, 1963).

[20]F. D. Feiock and W. F. Johnston, Phys. Rev. **187**, 39 (1969).

[21]J. van Kranendonk, Physica **20**, 781 (1954).

[22]R. L. Mieher, Phys. Rev. **125**, 1537 (1962).

[23]I. P. Goudemond, J. M. Keartland, and M. J. R. Hoch, J. Low Temp. Phys. **82**, 369 (1991).

[24]E. H. Hygh and T. P. Das, Phys. Rev. **143**, 452 (1966).